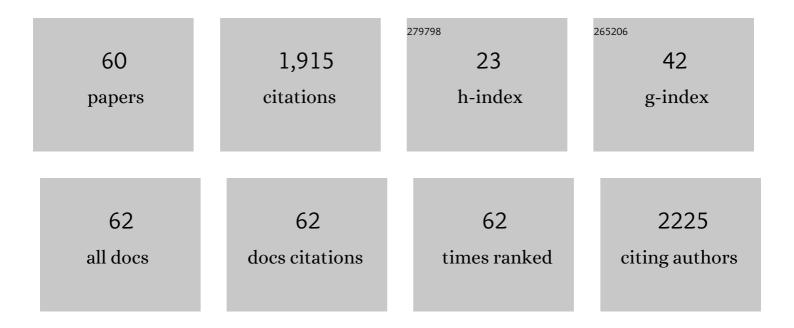
List of Publications by Year in descending order

Source: https://exaly.com/author-pdf/7771048/publications.pdf Version: 2024-02-01



#	Article	IF	CITATIONS
1	Ultrathin NiCo-MOF Nanosheets for High-Performance Supercapacitor Electrodes. ACS Applied Energy Materials, 2019, 2, 2063-2071.	5.1	319
2	Acetylene black enhancing the electrochemical performance of NiCo-MOF nanosheets for supercapacitor electrodes. Applied Surface Science, 2019, 492, 455-463.	6.1	126
3	Self-assembly carbon dots for powerful solar water evaporation. Carbon, 2019, 149, 556-563.	10.3	109
4	Coal tar pitch derived N-doped porous carbon nanosheets by the in-situ formed g-C3N4 as a template for supercapacitor electrodes. Electrochimica Acta, 2018, 283, 132-140.	5.2	92
5	Microstructural evolution and oxidation resistance of polyacrylonitrile-based carbon fibers doped with boron by the decomposition of B4C. Carbon, 2013, 56, 296-308.	10.3	71
6	Exfoliated graphite as a flexible and conductive support for Si-based Li-ion battery anodes. Carbon, 2014, 72, 38-46.	10.3	71
7	N-doped porous carbon anchoring on carbon nanotubes derived from ZIF-8/polypyrrole nanotubes for superior supercapacitor electrodes. Applied Surface Science, 2018, 457, 1018-1024.	6.1	71
8	Dynamic restructuring of carbon dots/copper oxide supported on mesoporous hydroxyapatite brings exceptional catalytic activity in the reduction of 4-nitrophenol. Applied Catalysis B: Environmental, 2020, 263, 118299.	20.2	62
9	Urchin-like Ni1/3Co2/3(CO3)0.5OH·0.11H2O anchoring on polypyrrole nanotubes for supercapacitor electrodes. Electrochimica Acta, 2019, 295, 989-996.	5.2	57
10	Microstructure and thermal/mechanical properties of short carbon fiber-reinforced natural graphite flake composites with mesophase pitch as the binder. Carbon, 2013, 53, 313-320.	10.3	56
11	Carbonâ€Dotâ€Based Heterojunction for Engineering Bandâ€Edge Position and Photocatalytic Performance. Small, 2018, 14, e1803447.	10.0	53
12	Carbon dots-stabilized Cu4O3 for a multi-responsive nanozyme with exceptionally high activity. Chemical Engineering Journal, 2020, 394, 125045.	12.7	43
13	In-situ incorporation of carbon dots into mesoporous nickel boride for regulating photocatalytic activities. Carbon, 2018, 137, 484-492.	10.3	42
14	A Cu2O-CDs-Cu three component catalyst for boosting oxidase-like activity with hot electrons. Chemical Engineering Journal, 2020, 382, 122484.	12.7	41
15	In-Situ Preparation of Boron-Doped Carbons with Ordered Mesopores and Enhanced Electrochemical Properties in Supercapacitors. Journal of the Electrochemical Society, 2012, 159, E177-E182.	2.9	38
16	Nitrogen-doped carbon dots encapsulated in the mesoporous channels of SBA-15 with solid-state fluorescence and excellent stability. Nanoscale, 2019, 11, 7247-7255.	5.6	34
17	Fluorine-free superhydrophobic carbon-based coatings on the concrete. Materials Letters, 2019, 244, 31-34.	2.6	33
18	Microstructure and thermophysical properties of B4C/graphite composites containing substitutional boron. Carbon, 2013, 52, 10-16.	10.3	32

#	Article	IF	CITATIONS
19	Multiscale carbon nanosphere–carbon fiber reinforcement for cement-based composites with enhanced high-temperature resistance. Journal of Materials Science, 2015, 50, 2038-2048.	3.7	32
20	Facile Synthesis of Carbon Dots@2D MoS ₂ Heterostructure with Enhanced Photocatalytic Properties. Inorganic Chemistry, 2019, 58, 5746-5752.	4.0	31
21	Lattice-Coupled Si/MXene Confined by Hard Carbon for Fast Sodium-Ion Conduction. ACS Applied Energy Materials, 2021, 4, 7268-7277.	5.1	29
22	Constructing mild expanded graphite microspheres by pressurized oxidation combined microwave treatment for enhanced lithium storage. Rare Metals, 2021, 40, 837-847.	7.1	29
23	Highly microporous graphite-like BC _x O _{3â^³x} /C nanospheres for anode materials of lithium-ion batteries. Journal of Materials Chemistry A, 2017, 5, 2835-2843.	10.3	25
24	Fabrication of boron-doped carbon fibers by the decomposition of B4C and its excellent rate performance as an anode material for lithium-ion batteries. Solid State Sciences, 2015, 41, 36-42.	3.2	24
25	A sandwich structure graphite block with excellent thermal and mechanical properties reinforced by in-situ grown carbon nanotubes. Carbon, 2013, 51, 427-430.	10.3	23
26	Cross-Linked Nanohybrid Polymer Electrolytes With POSS Cross-Linker for Solid-State Lithium Ion Batteries. Frontiers in Chemistry, 2018, 6, 186.	3.6	20
27	Boosting photocatalytic activity through in-situ phase transformation of bismuth-based compounds on carbon dots and quantification analysis of intrinsically reactive species in photocatalysis. Carbon, 2020, 165, 175-184.	10.3	20
28	Crystalline borophene quantum dots and their derivative boron nanospheres. Materials Advances, 2021, 2, 3269-3273.	5.4	20
29	Rational construction of densely packed Si/MXene composite microspheres enables favorable sodium storage. Rare Metals, 2022, 41, 1626-1636.	7.1	20
30	Lanthanide-doped LaOBr nanocrystals: controlled synthesis, optical spectroscopy and bioimaging. Journal of Materials Chemistry B, 2017, 5, 4827-4834.	5.8	19
31	Fabrication and supercapacitive properties of Fe2O3@C nanocomposites. Materials Letters, 2012, 80, 121-123.	2.6	18
32	A facile route for PbO@C nanocomposites: An electrode candidate for lead-acid batteries with enhanced capacitance. Journal of Power Sources, 2013, 224, 125-131.	7.8	17
33	PbTe nanodots confined on ternary B2O3/BC2O/C nanosheets as electrode for efficient sodium storage. Journal of Power Sources, 2020, 461, 228110.	7.8	16
34	Origin of sonocatalytic activity of fluorescent carbon dots. Carbon, 2021, 184, 102-108.	10.3	16
35	Incorporating quantum-sized boron dots into 3D cross-linked rGO skeleton to enable the activity of boron anode for favorable lithium storage. Chemical Engineering Journal, 2021, 425, 130659.	12.7	16
36	Photothermal, photocatalytic, and anti-bacterial Ti-Ag-O nanoporous powders for interfacial solar driven water evaporation. Ceramics International, 2021, 47, 19800-19808.	4.8	15

#	Article	IF	CITATIONS
37	Electronic and photocatalytic properties of modified MoS2/graphene quantum dots heterostructures: A computational study. Applied Surface Science, 2019, 473, 70-76.	6.1	14
38	Pore structure engineering of wood-derived hard carbon enables their high-capacity and cycle-stable sodium storage properties. Electrochimica Acta, 2021, 391, 139000.	5.2	13
39	Atomic Fe–N ₅ catalytic sites embedded in N-doped carbon as a highly efficient oxygen electrocatalyst for zinc–air batteries. Materials Chemistry Frontiers, 2021, 5, 8127-8137.	5.9	13
40	Structural evolution of rayon-based carbon fibers induced by doping boron. RSC Advances, 2014, 4, 59150-59156.	3.6	12
41	Highly microporous SbPO ₄ /BC _{<i>x</i>} hybrid anodes for sodium-ion batteries. Materials Advances, 2020, 1, 206-214.	5.4	12
42	Structural and electronic properties of effective p-type doping WS 2 monolayers: A computational study. Solid State Communications, 2018, 269, 58-63.	1.9	11
43	Constructing a Grape-like Silicon/Mildly Expanded Graphite Microsphere Composite as a High-Performance Anode Material for Lithium-Ion Batteries. Energy & Fuels, 2021, 35, 806-815.	5.1	9
44	Facile synthesis of polymer monolith functionalized with layered double hydroxide as effective preconcentration materials for fluorescent whitening agents. Microchemical Journal, 2017, 132, 93-99.	4.5	8
45	Three-dimensional B-doped porous carbon framework anchored with ultrasmall PbO/Pb nanocrystals for lithium storage. Ceramics International, 2017, 43, 12442-12451.	4.8	8
46	Expansive Behavior in Circular Steel Tube Stub Columns of SCC Blended with CFB Bottom Ashes. Journal of Materials in Civil Engineering, 2019, 31, .	2.9	8
47	The reaction behavior of carbon fibers and TaC at high temperatures. CrystEngComm, 2013, 15, 6928.	2.6	7
48	Green, energy-efficient preparation of CDs-embedded BiPO4 heterostructure for better light harvesting and conversion. Chemical Engineering Journal, 2020, 391, 123551.	12.7	7
49	Highly improved mechanical performances of polyvinyl butyral through fluorescent carbon dots. Materials Letters, 2020, 280, 128537.	2.6	7
50	The structure of MB2MCC (MZr, Hf, Ta) multi-phase ceramic coatings on graphite. Journal of the European Ceramic Society, 2014, 34, 2895-2904.	5.7	6
51	Hierarchical porous carbon fiber for fiber-shaped supercapacitor. Functional Materials Letters, 2021, 14, 2150016.	1.2	6
52	AlP-regulated phosphorus vacancies over Ni–P compounds promoting efficient and durable hydrogen generation in acidic media. Dalton Transactions, 2022, 51, 4033-4042.	3.3	6
53	Bottom-up synthesized crystalline boron quantum dots with nonvolatile memory effects through one-step hydrothermal polymerization of ammonium pentaborane and boric acid. CrystEngComm, 2022, 24, 3469-3474.	2.6	5
54	Molybdenum Selenide/Porous Carbon Nanomaterial Heterostructures with Remarkably Enhanced Light-Boosting Peroxidase-like Activities. ACS Applied Materials & Interfaces, 2021, 13, 54274-54283.	8.0	4

#	Article	IF	CITATIONS
55	TiO2 modification with multi-acid treatment for efficient interfacial perovskite-TiO2 electron transport. Journal of Alloys and Compounds, 2022, 898, 162837.	5.5	4
56	Richly electron-deficient BC _{<i>x</i>} O _{3â^'<i>x</i>} anodes with enhanced reaction kinetics for sodium/potassium-ion batteries. Materials Chemistry Frontiers, 2022, 6, 1882-1894.	5.9	4
57	A simple, scalable approach for combining carbon dots with hexagonal nanoplates of nickel-based compounds for efficient photocatalytic reduction. Dalton Transactions, 2018, 47, 12694-12701.	3.3	3
58	Preparation and Thermal Characterization of Hollow Graphite Fibers/Paraffin Composite Phase Change Material. Coatings, 2022, 12, 160.	2.6	2
59	Preparation and Electrochemical Properties of Pt@C Nanocomposites. Chemistry Letters, 2009, 38, 260-261.	1.3	1
60	Secondary granulation-assisted CVD growth of WS2, TiS2 and NbS2 crystals. Functional Materials Letters, 2021, 14, 2151029.	1.2	1